Ideal magnetohydrodynamic ballooning stability boundaries in three-dimensional equilibria[a)]

C. C. Hegna[b)]
Department of Engineering Physics, University of Wisconsin, Madison, Wisconsin 53706-1687

S. R. Hudson
Princeton Plasma Physics Laboratory, Princeton, New Jersey 08543

(Received 25 October 2001; accepted 29 November 2001)

The impact of three-dimensional geometry on ideal magnetohydrodynamic ballooning mode stability is studied. By using a class of ''local 3D equilibria'' [C. C. Hegna, Phys. Plasmas **7**, 3921 (2000)], the effects of plasma shaping, profile variations and symmetry on local plasma physics properties can be addressed. As an example, a local helical axis equilibrium case is constructed that models the magnetic field spectrum of a quasihelically symmetric stellarator. In this case, the magnetic harmonic structure of the local shear (which can be manipulated via changes in the magnetic geometry) has an important impact on the stability boundaries and eigenvalue properties of three-dimensional equilibria. The presence of symmetry breaking components in the local shear produces localized field-line-dependent ballooning instabilities in regions of small average shear. These effects lower first ballooning stability thresholds and can eliminate the second stability regime. A geometric interpretation of these results is given. © *2002 American Institute of Physics.* [DOI: 10.1063/1.1446037]

I. INTRODUCTION

Understanding the physical processes that limit the plasma stored energy in three-dimensional (3D) configurations is one of the principal tasks to be addressed in stellarator research. In theoretical studies of particular configurations, local criterion deduced from ideal magnetohydrodynamic (MHD) ballooning and Mercier mode theory are often used to predict β-limits of stellarators.[1–7] In this paper, we use local 3D equilibria[8] to study generic ideal MHD ballooning stability properties of three-dimensional configurations. Previous calculations[9] have shown that the presence of three-dimensional effects can have dramatic effects on ballooning stability boundaries. In this work, we expand upon this study through an examination of the field line dependence of the ballooning mode eigenvalue and show how this impacts the ability to find second ideal MHD ballooning stability regimes.

The difficult aspect of studying the role of three-dimensional shaping on local mode properties is the generation of three-dimensional equilibria. There is no rigorous proof of the existence of three-dimensional equilibria with nested topologically toroidal magnetic surfaces.[10] In general, global solutions to the magnetostatic equilibrium equations require numerical calculations. Using a computational approach to perform profile and parameters scans of three-dimensional equilibria is time consuming if not impossible since there is no general procedure for specifying 3D equilibria. This is in contrast to studies of symmetric systems where Grad–Shafranov theory guarantees the existence of toroidal equilibria. Methods have been developed to study the effect of axisymmetric shaping and profile variations on local mode stability for applications to tokamaks by generating sequences of solutions to the Grad–Shafranov equation local to a magnetic surface of interest.[11–13] These studies have been extended to three-dimensional systems by explicitly solving the three-dimensional MHD equilibria equations on a particular magnetic surface.[8,14] By application of this technique, one is able to construct stability boundaries for modes localized to magnetic surfaces as functions of three-dimensional shaping parameters and plasma profiles. An example of this analysis allows generation of generalized $\hat{s}-\alpha$ curves to denote stability boundaries as functions of plasma profiles where $\hat{s}$ and α are respectively dimensionless measures of the flux surface averaged magnetic shear and pressure gradient.[9,11,12]

There are important differences in the theory of ideal MHD ballooning modes in three-dimensional configurations with respect to axisymmetric devices. Using the conventional WKB-ballooning formalism in the short wavelength limit, the ballooning equation appears as an ordinary differential equation to be solved on each field line for a given radial wave number in the incompressible limit.[15] This results in a local dispersion relation for the ballooning equation eigenvalue as a function of magnetic surface, field line and wave vector. The characteristics of the associated eikonal equation can be written in Hamiltonian form. If the configuration under consideration has a continuous symmetry, the ballooning eigenvalue is independent of field line. In this case, the corresponding Hamiltonian equations are integrable and the WKB quantization condition can be used to predict the ballooning mode spectrum. However, for three-dimensional configurations, this is not the case and the use of

[a)]Paper BI1 4, Bull. Am. Phys. Soc. **46**, 20 (2001).
[b)]Invited speaker. Electronic mail: hegna@cptc.wisc.edu

a local dispersion relation to estimate the instability threshold is problematic.[15]

The field line dependence of the local ballooning eigenvalue is unique to three-dimensional systems. This dependence appears when the geometrical coefficients of the ballooning equation are functions of at least two helical angle coordinates of incommensurate helicity. In this case, the ballooning equation eigenmode becomes localized along the field line even in the limit of zero average shear ($\hat{s}=0$).[9,16] This behavior, as pointed out by Dewar and co-workers,[16,17] resembles the Anderson localization process of solid state physics where electron transport is inhibited by localized electron wave functions due to the presence of impurities on an otherwise periodic lattice.[18] Anderson localized modes have a remarkable effect on ballooning stability boundaries as measured by generalized $\hat{s}-\alpha$ curves of the ballooning mode theory.[9] In particular, the presence of a symmetry breaking contribution to the local shear for a model quasihelically symmetric configuration lowers the critical gradient in the first stability regime and can eliminate the second stability region.

In Sec. II, the construction of local 3D equilibria is introduced and a particular example of the model is parametrized. Ballooning stability calculations for this model are carried out in Sec. III. A discussion of the results is given in Sec. IV.

II. LOCAL HELICAL AXIS EQUILIBRIA

The motivation for using local equilibria is to avoid the necessity of constructing global solutions to the three-dimensional magnetostatic equilibrium equations. Calculations of global solutions to the 3D MHD equilibria problem are nontrivial; however, for calculating the local eigenvalues of ballooning stability theory, only equilibrium information on the magnetic surface is required.

Local equilibria are prescribed by two sets of data: (1) two profile quantities, and (2) the shape of the magnetic field line trajectories on the magnetic surface ψ_0. In this work, the two profile quantities are choosen to be the pressure gradient $dp/d\psi$ and rotational transform gradient $d\iota/d\psi$ at the magnetic surface where ψ is the toroidal flux function that labels the magnetic surfaces. Alternatively, one could choose the net parallel current as one of the free functions and determine $d\iota/d\psi$ from the current and pressure gradient by taking the appropriate flux surface average of an identity relating the local shear to plasma current and shaping effects [see Eq. (6)].

The three-dimensional shaping is specified by the inverse magnetic coordinate mapping function $\mathbf{X}(\theta,\zeta)$ and the rotational transform ι_0 on the magnetic surface labeled by $\psi=\psi_0$. Here, θ and ζ are, respectively, any choice of straight-field-line poloidal and toroidal angles [the magnetic field is written $\mathbf{B}=\nabla\psi\times\nabla(\theta-\iota\zeta)$]. We refer to these data as the magnetic geometry since it completely specifies the trajectory of a magnetic field line on the magnetic surface. In particular, the unit tangent vector $\hat{\mathbf{b}}$ given by

$$\hat{\mathbf{b}}\equiv\frac{\partial_\zeta\mathbf{X}+\iota_0\partial_\theta\mathbf{X}}{|\partial_\zeta\mathbf{X}+\iota_0\partial_\theta\mathbf{X}|} \tag{1}$$

and unit normal vector $\hat{\mathbf{n}}$ given by

$$\hat{\mathbf{n}}\equiv\frac{\partial_\theta\mathbf{X}\times\partial_\zeta\mathbf{X}}{|\partial_\theta\mathbf{X}\times\partial_\zeta\mathbf{X}|}=\frac{\nabla\psi}{|\nabla\psi|} \tag{2}$$

are calculated from derivatives of $\mathbf{X}(\theta,\zeta)$, where $\partial_\theta\mathbf{X}\equiv\partial\mathbf{X}/\partial\theta$ and $\partial_\zeta\mathbf{X}\equiv\partial\mathbf{X}/\partial\zeta$. Knowledge of $\mathbf{X}(\theta,\zeta)$ allows one to calculate key geometric quantities associated with the magnetic field, such as the normal, κ_n, and geodesic, κ_g, curvatures which enter in pressure driven instability studies. These are given by

$$\kappa_n=\hat{\mathbf{n}}\cdot(\hat{\mathbf{b}}\cdot\nabla)\hat{\mathbf{b}}, \tag{3}$$

$$\kappa_g=\hat{\mathbf{b}}\times\hat{\mathbf{n}}\cdot(\hat{\mathbf{b}}\cdot\nabla)\hat{\mathbf{b}}. \tag{4}$$

An additional magnetic geometry quantity is the normal torsion (''twist'' of the field lines) given by

$$\tau_n=-\hat{\mathbf{n}}\cdot(\hat{\mathbf{b}}\cdot\nabla)(\hat{\mathbf{b}}\times\hat{\mathbf{n}}), \tag{5}$$

which is also important in ballooning theory since it enters in the relation for determining the local shear. The local shear $s=(\hat{\mathbf{b}}\times\hat{\mathbf{n}})\cdot\nabla\times(\hat{\mathbf{b}}\times\hat{\mathbf{n}})$ is related to the normal torsion and parallel current by the identity

$$s=\frac{\mathbf{J}\cdot\mathbf{B}}{B^2}-2\tau_n, \tag{6}$$

using $\hat{\mathbf{n}}\cdot\nabla\times\hat{\mathbf{n}}=0$ where the parallel current is the sum of the net current and the Pfirsch–Schlüter current,

$$\frac{\mathbf{J}\cdot\mathbf{B}}{B^2}=\sigma+\frac{dp}{d\psi}\lambda. \tag{7}$$

The quantity $\sigma=\langle\mathbf{J}\cdot\mathbf{B}\rangle/\langle B^2\rangle$ is constant on the magnetic surface, $dp/d\psi$ is the pressure gradient and the Pfirsch–Schlüter coefficient, λ, is calculated from the magnetic differential equation,

$$\mathbf{B}\cdot\nabla\lambda=2\kappa_g\frac{|\nabla\psi|}{B}, \tag{8}$$

where all the terms on the right-hand side are determined from $\mathbf{X}(\theta,\zeta)$.[8] A constraint on the parametrization is that solutions to magnetic differential equations, such as Eq. (8), avoid ''small denominators'' that appear at rational surfaces by either considering a magnetic surface with an irrational value of ι_0 or demand that the magnetic field geometry parametrization, $\mathbf{X}(\theta,\zeta)$, not produce resonant Fourier components if ι_0 is rational. Global solutions to the MHD equilibrium equations in three dimensions require that singular solutions be avoided at every rational surface. This strong constraint is the underlying reason why 3D MHD equilibria solutions with finite pressure are difficult to obtain.[19] Since only a single surface is needed in this work, the singular current problem is not as serious an issue here.

In this work, we consider a specific case that models a magnetic surface in a quasihelically symmetric configuration,[20] where a single Fourier harmonic dominates

the magnetic field spectrum.[21] In particular, the inverse mapping quantity $\mathbf{X}(\theta,\zeta)$ is specified in cylindrical coordinates $[R,\phi,Z]=[R(\theta,\zeta),-\zeta,Z(\theta,\zeta)]$ by

$$R=R_0+\rho_0\cos(\theta)+\Delta\cos(N\zeta)+\frac{2R_0\rho_0}{N^2\Delta}\sin(N\zeta)\sin(\theta), \tag{9}$$

$$Z=\rho_0\sin(\theta)+\Delta\sin(N\zeta)-\frac{2R_0\rho_0}{N^2\Delta}\sin(N\zeta)\cos(\theta), \tag{10}$$

where the length scales Δ, R_0, and ρ_0 and the toroidal periodicity parameter N are input to the local equilibria geometry. While more general cases exist, we concentrate on a particular limit that models a quasihelically symmetric equilibria. The orderings $N^2\Delta/R_0\gg 1>N\Delta/R_0$ and $\rho_0\sim\Delta$ are used. In this case, the magnetic surface is circular to lowest order with the center of the circle rotating with the helical pitch $N\zeta-\theta$. The last terms in Eqs. (9) and (10) give small mirror-like corrections that beat with the helical symmetric angle to cancel out the toroidal curvature to leading order. This has the effect of producing a curvature vector, magnetic field spectrum and Pfirsch–Schlüter current spectrum that are dominated by the helical angle $N\zeta-\theta$, as one would find in a quasihelically symmetric configuration.[20]

From Eqs. (1) to (4), the normal and geodesic curvatures are given by

$$\kappa_n=-\frac{N^2\Delta}{R_0^2}\cos(N\zeta-\theta)-\frac{1}{R_0}\cos(2N\zeta-\theta)+\mathcal{O}\left(\frac{1}{N^2\Delta}\right), \tag{11}$$

$$\kappa_g=-\frac{N^2\Delta}{R_0^2}\sin(N\zeta-\theta)\left[1+\frac{N^2\Delta^2}{R_0^2}\right]+\frac{2\rho_0}{R_0}\sin(N\zeta)-\frac{1}{R_0}\sin(2N\zeta-\theta)+\mathcal{O}\left(\frac{1}{N^2\Delta}\right), \tag{12}$$

and are dominated by a single harmonic in the asymptotic limit $N^2\Delta\gg R_0$ $[\kappa_n\approx-(N^2\Delta/R_0^2)\cos(N\zeta-\theta)$, $\kappa_g\approx-(N^2\Delta/R_0^2)\sin(N\zeta-\theta)]$. From Eq. (5), the normal torsion is given by

$$\tau_n=-\frac{2}{N\Delta}\cos(N\zeta)+\frac{\iota_0}{R_0}-\frac{N^3\Delta^2}{R_0^3}\cos^2(N\zeta-\theta)+\mathcal{O}\left(\frac{1}{N^2\Delta}\right). \tag{13}$$

Unlike components of the curvature vector, the normal torsion is not dominated by a single harmonic. We argue that the properties described in the geometric expressions for the local helical axis case are generic for all quasisymmetric configurations. A considerable amount of work in the stellarator community has been spent on three-dimensional configurations with quasisymmetry since neoclassical transport is predicted to be superior to the equivalent conventional stellarator.[21] While attention is paid to controlling the magnetic field spectrum and hence components of the curvature vector in these studies, no particular requirements are imposed on the normal torsion. Therefore, for general three-dimensional equilibria, the normal torsion is a three-dimensional function of space and does not share the same symmetry properties as the magnetic field.

Following the procedure of Ref. 8, the Jacobian $(\equiv 1/\nabla\psi\times\nabla\theta\cdot\nabla\zeta)$, field strength and $|\nabla\psi|^2$ can be calculated. For this case, these are given by

$$\sqrt{g}=\hat{V}'\left[1+\frac{N^2\Delta\rho_0}{R_0^2}\cos(N\zeta-\theta)+\mathcal{O}\left(\frac{\Delta}{R_0}\right)\right], \tag{14}$$

$$B^2=\frac{R_0^2}{(\sqrt{g})^2}\left[1+\mathcal{O}\left(\frac{N^2\Delta^2}{R_0^2}\right)\right], \tag{15}$$

$$|\nabla\psi|^2=\frac{\rho_0^2R_0^2}{(\sqrt{g})^2}\left[1+\mathcal{O}\left(\frac{N^2\Delta^2}{R_0^2}\right)\right], \tag{16}$$

where $\hat{V}'$ is an overall normalization constant.[8] Using Eqs. (8), (12), (14)–(16), the Pfirsch–Schlüter coefficient, λ, is derived and given by

$$\lambda=\frac{2\rho_0\hat{V}'\Delta}{R_0^2}\frac{N^2}{N-\iota_0}\left[\cos(N\zeta-\theta)-\frac{2\rho_0R_0}{N^2\Delta^2}\cos(N\zeta)+\frac{R_0}{2N^2\Delta}\cos(2N\zeta-\theta)+\mathcal{O}\left(\frac{\Delta}{R}\right)\right], \tag{17}$$

which is dominated by a single harmonic in the asymptotic limit $N^2\Delta\gg R_0$: $\lambda\approx-[2\rho_0\Delta\hat{V}N^2/R_0^2(N-\iota)^2]\cos(N\zeta-\theta)$.

In the limit $N^2\Delta/R_0\gg 1$, the curvature vector, field strength, and Pfirsch–Schlüter current are dominated by the single helical harmonic $N\zeta-\theta$. These quantities are related in MHD equilibrium theory. However, note that the normal torsion contains a large Fourier component with incommensurate helicity to the harmonic that dominates the curvature. Namely, the first term in Eq. (13) represents a mirroring term that enters at leading order. It is the presence of this term in the expression for the local shear that produces a dramatic effect on the ballooning stability properties of this equilibria relative to a completely symmetric equilibrium.

III. BALLOONING STABILITY

A standard ballooning WKB-like ansatz is used to describe the ideal MHD plasma displacement, $\Xi\sim e^{iS(\mathbf{x})\epsilon^{-1}}\xi(\mathbf{x})$, where $\epsilon\ll 1$ and $S(\mathbf{x})$ and $\xi(\mathbf{x})$ vary as order unity quantities in space. The property $\mathbf{B}\cdot\nabla S=0$ (which is consistent with $k_\parallel/k_\perp\sim\epsilon\ll 1$) with $\mathbf{B}=\nabla\psi\times\nabla(\zeta-\iota\theta)$, implies S can be written $S=\zeta-\iota\theta+f(\psi)$ where ι is constant on the magnetic surface when ζ and θ are straight-field-line angles. To leading order in the small parameter ϵ, the eigenfunction satisfies

$$\mathbf{B}\cdot\nabla\left(\frac{|\nabla S|^2}{B^2}\mathbf{B}\cdot\nabla\xi\right)+\frac{dp}{d\psi}\frac{1}{|\nabla\psi|}(\kappa_n+\kappa_g\Lambda)=-\rho_M\frac{|\nabla S|^2}{B^2}\omega^2\xi, \tag{18}$$

for the local eigenvalue ω^2 where ρ_M is the mass density on the magnetic surface and incompressibility is assumed.[15] The quantity $|\nabla S|^2$ contains the effect of magnetic shear. This quantity is written

$$|\nabla S|^2 = \frac{B^2}{|\nabla \psi|^2}(1+\Lambda^2), \tag{19}$$

where

$$\Lambda = \frac{|\nabla \psi|^2}{B}\int \frac{dl}{B}\frac{B^2}{|\nabla \psi|^2}s. \tag{20}$$

Applying the ordering $N^2\Delta/R_0 \gg 1 > N\Delta/R_0$ for the local helical axis case, the ballooning equation becomes

$$\frac{d}{d\eta}(1+\Lambda^2)\frac{d\xi}{d\eta} + \alpha[\cos(\eta)+\Lambda\sin(\eta)] = -\omega^2(1+\Lambda^2)\xi, \tag{21}$$

where $\eta = N\zeta - \theta$ labels points along the field line, $\Omega^2 = \omega^2\rho_M \hat{V}'^2/(N-\iota)^2$ is the normalized eigenvalue, $\alpha = -(dp/d\psi)(2\rho_0\Delta\hat{V}'/R_0)[N^2/(N-\iota)^2]$ is the normalized pressure gradient and

$$\Lambda(\eta,\chi) = \int_{\eta_k}^{\eta} d\eta[\hat{s}-\alpha\cos(\eta)+\tau_0\cos(2\eta) + \delta\cos(k\eta+k\chi)], \tag{22}$$

where $\hat{s} \equiv (d\iota/d\psi)[R_0\rho_0^2/\hat{V}'(N-\iota)]$, $\tau_0 = N^2\Delta^2/R_0^2$, $\delta = 4R_0/N(N-\iota)\Delta$, $k = N/(N-\iota)$, and $\chi \equiv \theta - \iota\zeta$ is the field line label. In the ordering scheme used here, the normal and geodesic curvatures are dominated by a single harmonic described by the first terms in Eqs. (11) and (12). However, the last term in $\Lambda(\eta, \chi)$ represents the three-dimensional property of the helical axis equilibria. This term arises from the first term of the expression for the normal torsion, Eq. (13). Note that this term is explicitly field line (χ) dependent and has incommensurate helicity with the helical symmetry angle.

Ideal MHD ballooning stability boundaries are present when the local eigenvalue satisfies $\Omega^2 = 0$. On the magnetic surface, the eigenvalue is a function of the radial eigenvector and field-line label: $\Omega^2 = \Omega^2(\eta_k, \chi)$. In the ballooning equation, five parameters describe the equilibria. Two of these parameters, $\hat{s}$ and α are, respectively, dimensionless measures of the rotational transform gradient and pressure gradient, and correspond to the two profile quantities required for specification of the local equilibria. The quantities τ_0, δ, and k come from the magnetic geometry specification. In the limit $\delta = \tau_0 = 0$, the ballooning equation has precisely the same mathematical structure as the shifted circle equilibria used in axisymmetric tokamak studies,[11] other than a scaling factor $\iota_0/(\iota_0 - N)$ which accounts for the proper connection length in normalizing $\hat{s}$ and α for helically symmetric geometry. In what follows, we set $\tau_0 = 0$ for simplicity. Non-zero values of τ_0 alter the stability boundaries quantitatively, however, the same general features of the $\tau_0 = 0$ case are seen since this term does not introduce symmetry breaking terms into the ballooning equation. The factor k is only relevant when $\delta \neq 0$. If the rotational transform ι_0 is irrational, $k = N/(N-\iota_0)$ is also irrational.

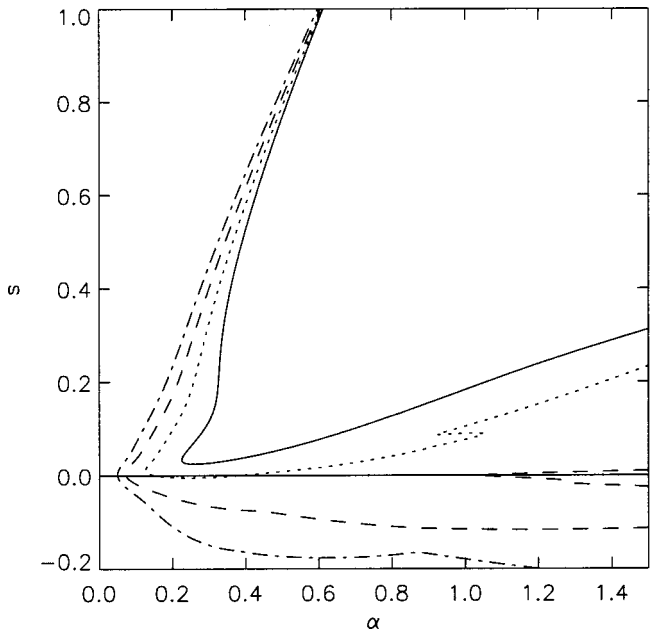

FIG. 1. Ideal MHD stability boundaries of the ballooning equation, Eq. (21), with $\tau_0 = 0$, and $k = \pi^2/8$ for different values of the symmetry breaking factor δ. The solid, dotted, dashed, and dashed–dotted curves correspond to $\delta = 0$, 0.15, 0.30, 0.45, respectively. For each value of δ, $\hat{s}$, and α a search is done over all possible values of the field line variable χ and η_k to find the most unstable eigenvalue. If at least one field line has an unstable local eigenvalue, the region of the $\hat{s}-\alpha$ parameter space is considered to be unstable.

The most important geometric modification to the three-dimensional is embodied in the contribution to the local shear proportional to δ. Solutions of the stability boundaries are plotted in Fig. 1 for a range of values for δ. The stability curves for the $\delta = 0$ case is equivalent to the standard symmetric tokamak-like case where for $\hat{s} > 0$ there are two marginal stability points at fixed $\hat{s}$ that demark the first and second stability regimes. As δ increases, generally the first stability boundary degrades. More strikingly, as δ increases there is a significant deterioration of the second stability regime, and for large enough δ there is only one ballooning stability boundary for a given $\hat{s}$. Additionally, ballooning instability can occur at $\hat{s} = 0$; the symmetry breaking variations in the local shear generally determine the stability boundaries in the small $\hat{s}$ region.

The behavior of the ballooning mode properties are different in the large-$\hat{s}$ [$\hat{s} \sim \mathcal{O}(1)$] region from the small-$\hat{s}$ region of parameter space. At large $\hat{s}$, the mode has a strong ballooning character; it is localized to a narrow region in η where the curvature is unfavorable. In this region, the average shear, $\hat{s}$, dominates other contributions to the local shear and is responsible for the localization along the field line. Since the symmetry breaking term, δ, does not play much of a role at large $\hat{s}$, the ballooning stability boundaries are weakly dependent upon δ.

In the small $\hat{s}$ region of symmetric tokamak-like configurations, the mode extent along η is large compared to 2π.

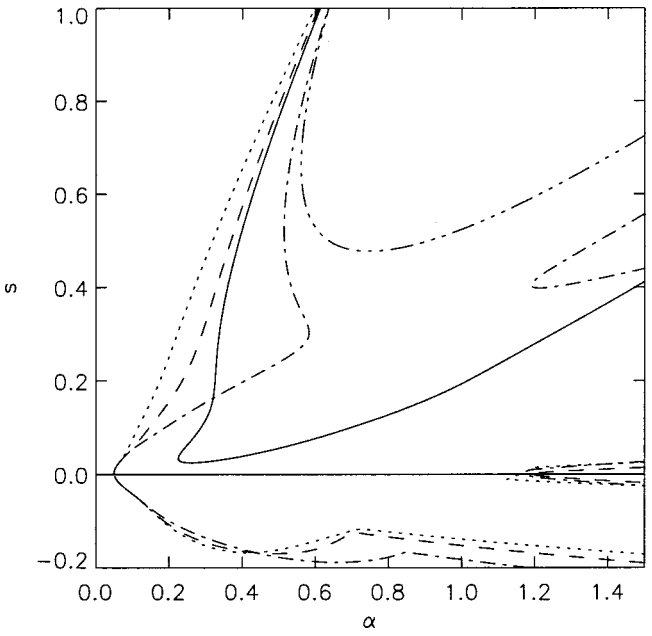

FIG. 2. Ideal MHD ballooning stability boundaries for fixed values of $\tau_0=0$, $k=\pi^2/8$, $\eta_k=0$, and $\delta=0.45$ at various choices of magnetic field line label. The solid line corresponds to the $\delta=0$ case where no symmetry breaking contribution is present and the local eigenvalues are independent of field line. The dotted, dashed, dashed–dotted, and dashed–triple-dotted curves correspond to $\chi=0$, 0.85, 1.70, 2.55, respectively with $\delta=0.45$. The presence of nonzero δ introduces a field line dependent local eigenvalue. Each field line has a dramatically different $\hat{s}-\alpha$ stability boundary indicating the general property that ballooning eigenvalues are field line dependent.

For this case, a multiple scale analysis can be applied to solve for the ballooning equation.[22] Using this technique, one finds that the mode structure is described by an oscillation along the field line, which describes the ballooning effect, modulating an extended envelope which has width $\mathcal{O}(1/\hat{s})$. An important aspect of this analysis is a description of the second stability region at large α. However, when symmetry breaking contributions to the local shear enter, the extended envelope feature of the mode shape is disrupted.[9] In the presence of non-zero δ, the mode tends to be more localized along η in the bad curvature regions. This has the property of lowering the first stability region and eliminating the second stability region at large enough δ.

Another aspect of three-dimensional equilibria is demonstrated in Fig. 2. In this figure, the solid curve represents the $\delta=0$ case corresponding to the symmetric case. The eigenvalues for this case are independent of field line label. The remainder of the stability curves correspond to the common value of $\delta=0.45$ (the magnetic geometry is fixed) for different magnetic field lines on the magnetic surface as labeled by the value of χ. In particular, for the field line choice $\chi=2.55$, all equilibria with $\hat{s}<0.5$ have stable ballooning eigenvalues. However, for the same magnetic geometry at the field line choice $\chi=0$, at sufficiently large α nearly every equilibrium is unstable for $\hat{s}>-0.2$. Generally speaking, in small $\hat{s}$ regions every magnetic surface contains a mixture of field lines with both stable and unstable local eigenvalues.

Cuthbert and Dewar pointed out that the effect of incommensurate helicities in general three-dimensional equilibria is to produce localized ballooning eigenfunctions even in small $\hat{s}$ regions.[16] What is demonstrated here is that these localized eigenfunctions can significantly effect the operational ballooning stability boundaries.[9]

IV. DISCUSSION

In this work, the role of symmetry in various magnetic geometry quantities is addressed for the ideal MHD ballooning stability properties of three-dimensional equilibria. The general features indicate that the presence of incommensurate helicities in the local shear and magnetic field line curvature produce localized eigenfunctions that can reduce ideal MHD ballooning mode instability thresholds and eliminate second stability regimes. An example of this behavior is explicitly demonstrated through the construction of local 3D equilibria[8] that model quasisymmetric configurations where the curvature is dominated by a single harmonic, while the local shear contains harmonics of incommensurate helicity. While a particular example is used to illustrate the ideal ballooning mode stability properties, we hypothesize that the observed behavior is somewhat generic to three-dimensional systems.

A geometric interpretation of these results can be identified. Ideal ballooning instabilities tend to emerge when regions of small local shear coincide with regions of unfavorable curvature. In axisymmetric tokamak systems, these regions are functions of poloidal angle only and ideal ballooning instabilities occur when the local shear is small on the low field side.[12] As the pressure gradient increases, the Pfirsch–Schlüter current modification of the local shear causes the small shear region to migrate from the outboard side towards a region away from the bad curvature. At large enough pressure gradient, the ideal ballooning mode is stabilized and the second stability regime arises. In a perfectly helically symmetric equilibrium, a similar behavior would be expected.[14] However, in three-dimensional configurations the situation is more complicated. As shown here, the presence of an incommensurate helical component of the local shear produces a configuration where the regions of small shear and unfavorable curvature overlap at distinct points on the magnetic surface. Since only particular field lines intersect these regions, the ballooning eigenvalues are much more field line dependent. Unlike the axisymmetric case, the Pfirsch–Schlüter current-induced modulation of the local shear cannot remove these regions in general; thus a configuration without a second stability regime results. This is particularly true in the small $\hat{s}$ region where the helical content of the local shear determines the stability boundaries.

The important practical question to be answered is: do the local stability criteria derived from the ballooning equation really determine the operational limits? Highly localized, field line dependent ballooning eigenmodes typically are the most susceptible to instability. Due to their highly localized structure they may not have practical implications for high-β stellarator operation. As pointed out in Ref. 15, constructions of global modes from the local ballooning properties of three-dimensional equilibria is problematic. Hence, the instability threshold of a true global mode of the

three-dimensional system may not correspond to the predicted instability threshold described by the local theory. Additionally, finite Larmor radius effects can also effect the stability properties of highly localized structures. It may be the case that the use of local MHD stability criterion to determine operational limits in stellarators is too pessimistic. We leave this speculation as a motivation for future work on this topic.

ACKNOWLEDGMENTS

The authors thank Dr. R. Torasso, R. L. Dewar, and J. D. Callen for useful discussions.

This work is supported by the U.S. Department of Energy under Contract No. DE-FG02-99ER54546.

[1]W. A. Cooper, Y. Nakamura, M. Wakatani *et al.*, in *Proceedings of the 19th European Physical Society Conference on Controlled Fusion and Plasma Physics*, Innsbruck, 1992 (European Physical Society, Petit-Lancy, Switzerland, 1992), ECA Vol. 10C, p. 557.
[2]R. Moeckli and W. A. Cooper, Nucl. Fusion **33**, 1899 (1993); Phys. Plasmas **1**, 793 (1994).
[3]W. A. Cooper and H. J. Gardner, Nucl. Fusion **34**, 729 (1994).
[4]J. A. Talmadge and W. A. Cooper, Phys. Plasmas **3**, 3713 (1996).
[5]N. Nakajima, Phys. Plasmas **3**, 4545 (1996); **3**, 4556 (1996).
[6]W. C. Cooper, Phys. Plasmas **7**, 2546 (2000).
[7]A. H. Reiman, L. Ku, D. A. Monticello *et al.*, Phys. Plasmas **8**, 2083 (2001).
[8]C. C. Hegna, Phys. Plasmas **7**, 3921 (2000).
[9]C. C. Hegna and S. R. Hudson, Phys. Rev. Lett. **87**, 035001 (2001).
[10]H. Grad, Phys. Fluids **10**, 137 (1967).
[11]J. W. Connor, R. J. Hastie, and J. B. Taylor, Phys. Rev. Lett. **40**, 396 (1978).
[12]J. M. Greene and M. S. Chance, Nucl. Fusion **32**, 453 (1981).
[13]R. L. Miller, M. S. Chu, J. M. Greene, Y. R. Lin-Liu, and R. E. Waltz, Phys. Plasmas **5**, 973 (1998).
[14]C. C. Hegna and N. Nakajima, Phys. Plasmas **5**, 1336 (1998).
[15]R. L. Dewar and A. H. Glasser, Phys. Fluids **26**, 3038 (1983).
[16]P. Cuthbert and R. L. Dewar, Phys. Plasmas **7**, 2302 (2000); P. Cuthbert, J. L. V. Lewandowski, H. J. Gardner *et al.*, *ibid.* **5**, 2921 (1998).
[17]R. L. Dewar, R. Ball, and P. Cuthbert, Phys. Rev. Lett. **86**, 2321 (2001).
[18]P. W. Anderson, Phys. Rev. **109**, 1492 (1958).
[19]W. A. Newcomb, Phys. Fluids **2**, 362 (1959).
[20]J. Nührenberg and R. Zille, Phys. Lett. A **114**, 129 (1986).
[21]A. H. Boozer, Phys. Fluids **23**, 904 (1980); **24**, 1999 (1981).
[22]R. D. Hazeltine and J. D. Meiss, *Plasma Confinement* (Addison–Wesley, Redwood City, 1992), pp. 309–312.